

# Negative-temperature Fourier transport in one-dimensional systems

Marco Baldovin<sup>1</sup> and Stefano Iubini<sup>2,3</sup>

<sup>1</sup>*Department of Physics, Università “Sapienza”, Roma Piazzale A. Moro 5, I-00185 Italy*

<sup>2</sup>*Consiglio Nazionale delle Ricerche, Istituto dei Sistemi Complessi,  
via Madonna del Piano 10, I-50019 Sesto Fiorentino, Italy*

<sup>3</sup>*Istituto Nazionale di Fisica Nucleare, Sezione di Firenze,  
via G. Sansone 1 I-50019 Sesto Fiorentino, Italy*

(Dated: February 28, 2025)

We investigate nonequilibrium steady states in a class of one-dimensional diffusive systems that can attain negative absolute temperatures. The cases of a paramagnetic spin system, a Hamiltonian rotator chain and a one-dimensional discrete linear Schrödinger equation are considered. Suitable models of reservoirs are implemented to impose given, possibly negative, temperatures at the chain ends. We show that a phenomenological description in terms of a Fourier law can consistently describe unusual transport regimes where the temperature profiles are entirely or partially in the negative-temperature region. Negative-temperature Fourier transport is observed both for deterministic and stochastic dynamics and it can be generalized to coupled transport when two or more thermodynamic currents flow through the system.

## I. INTRODUCTION

The characterization of steady states of open classical and quantum systems is a central problem in physics, with many implications both for theoretical studies and for applications. In the context of nonequilibrium statistical mechanics, the study of transport problems in simple low-dimensional lattices is a field which has been deeply investigated in the last decades. Relevant examples include the discovery of nonequilibrium phase transitions [1], anomalous transport [2] or mechanisms of dynamical arrest of transport [3].

In the typical nonequilibrium setup, the system is steadily driven out of equilibrium by external mechanical or thermodynamical forces. When the departure from equilibrium is sufficiently small, the usual assumption is that macroscopic currents are linearly related to the applied forces. The Fourier law is certainly one of the most celebrated examples of such phenomenological relations, where the heat current is proportional to the opposite of the temperature gradient, the proportionality constant being the thermal conductivity. Despite our understanding of the microscopic origin of Fourier law is still far from being complete, significant achievements have been made in the last years to explain its emergence or breakdown in low-dimensional systems [4].

In this paper, we focus on the problem of heat conduction for a peculiar class of models capable to attain negative absolute temperatures. Thermodynamics and statistical mechanics at negative absolute temperature have been quite a debated problem in the last decades. Since the pioneering studies by Onsager [5] and Ramsey [6], many theoretical and experimental results have been found. Recent examples include spin systems [7], vortices [8, 9] and cold atoms [10]. Although a general theoretical framework is reasonably well established for what concerns equilibrium thermodynamics and relaxation to equilibrium, the problem of steady transport in the presence of negative temperature states has received

much less attention. In [11] it was shown that a one-dimensional Discrete Nonlinear Schrödinger Equation in steady out-of-equilibrium conditions can spontaneously enter the negative-temperatures region even when the reservoirs impose positive temperatures at its boundaries. In this example, negative temperature states are obtained in the bulk of the system and are signaled by the emergence of localized structures (discrete breathers [12]) which act as bottlenecks and make the system a bad heat conductor. In this unusual situation, nonequilibrium negative temperature states are characterized by strong energy fluctuations and occur when large imbalances are imposed at the boundary of the chain.

On a more general ground, several fundamental questions concerning heat transport at negative temperatures still need to be clarified. For example: can diffusive transport at negative temperatures be described by a Fourier law for sufficiently small thermal imbalances? What are the properties of the related stationary states? Here we shed some light on these issues by studying both deterministic and stochastic systems driven out of equilibrium by possibly negative-temperature imbalances.

We start from one of the simplest systems satisfying our requirements, i.e. a paramagnetic chain of spins evolving according to stochastic local updates that conserve the total energy. Due to the absence of interaction terms in the Hamiltonian, analytical expressions for the stationary temperature profiles and for the thermal conductivity can be derived. We also show that the passage from the infinite temperature point does not pose any intrinsic limit to the Fourier problem. Indeed we show that stationary states where the inverse temperature profile changes its sign are consistently described. We then move to the study of a deterministic Hamiltonian system, namely the case of a chain of coupled rotators with bounded kinetic energy [13–15]. In this case, we show that transport is diffusive and that the regime of negative-temperature Fourier transport is accessible as well. Finally, we consider a slightly more complex

situation where negative-temperature steady states are obtained in conditions of coupled transport, i.e. when two independent currents are steadily sustained in the system as in thermoelectricity. Specifically, we analyze the case of a mixed deterministic-stochastic Schrödinger equation, a model recently introduced as a particularly simple example where (diffusive) coupled transport arises in a harmonic chain of coupled complex oscillators subject to conservative noise [16].

To investigate this peculiar transport setup, we need to introduce the interaction of the system with suitable boundary reservoirs that can sustain negative temperatures. As usual, a reservoir is a very large (ideally infinite) system that can either release or absorb energy without modifying its thermodynamical state. For the spin system we introduce a simple implementation of stochastic reservoir, while for deterministic systems we make use of generalized Langevin equations as discussed in [15].

The paper is organized as follows. In Sec. II we review some general properties of the nonequilibrium setup in one-dimensional systems and discuss a formulation of the Fourier law that is naturally extendable to the case of negative-temperature heat conduction. In Sec. III we analyze the case of heat conduction in a spin chain, while Sec.s IV and V we discuss the cases of the Hamiltonian rotator chain and the linear-stochastic Schrödinger equation, respectively. Finally, Sec. VI is devoted to conclusions and to a brief summary of open problems.

## II. FOURIER LAW AND TEMPERATURE PROFILES AT NEGATIVE TEMPERATURE

The study of one-dimensional models whose boundaries are kept at some fixed temperatures  $T_L$  and  $T_R$ , with  $T_R \neq T_L$ , is far from being a trivial task, and it is usually difficult to provide a satisfactory theoretical explanation for the observed phenomenology [2, 4, 17]. A relatively simple situation is represented by systems which are close to equilibrium, i.e. whose boundary temperatures are almost equal: in this case it is reasonable to expect that, after a suitable thermalization time, the system will be found in a stationary state in which a local-equilibrium condition is satisfied, and the average energy flux  $j$  does not depend on the position  $x$ . If an explicit relation between  $j$ , the temperature and its gradient is known, from the condition

$$j(T(x), \partial_x T(x)) = \text{const}, \quad (1)$$

it is clearly possible to get an equation for the temperature profile. Such an explicit relation is usually not known, but one can still rely on the empirical Fourier law

$$j = -\kappa(T)\partial_x T, \quad (2)$$

where  $\kappa(T)$  is the thermal conductivity; if  $T_R$  and  $T_L$  are close enough,  $\kappa(T)$  can be considered constant along

the system, so that a linear temperature profile can be expected. It is worth noticing that the same reasoning can be repeated in terms of the inverse temperature  $\beta = 1/k_B T$  (in the following we put the Boltzmann constant  $k_B$  equal to 1). From Eq. (2) one gets

$$j = \frac{\kappa(1/\beta)}{\beta^2} \partial_x \beta = \gamma(\beta) \partial_x \beta, \quad (3)$$

where  $\gamma = \kappa/\beta^2$  is the associated thermal transport coefficient: if the relative difference between  $T_R$  and  $T_L$  is small, also  $\gamma(\beta(x))$  is almost constant along the chain, and the above equation insures that the  $\beta$  profile, not surprisingly, is almost linear as well.

In the following, we will argue that Eq. (3) provides a consistent description of Fourier transport even in the regime of negative temperatures. In this respect we recall that, as already stated in the seminal paper by Ramsey [6], the introduction of negative temperatures does not affect the basic principle “heat flows from hot to cold”, provided that the temperature scale is expressed in terms of  $\beta$  instead of  $T$ . As a consequence, one might reasonably expect that the qualitative behaviour of these systems is still described by Eq. (3) when they are driven out of equilibrium from thermal baths at the boundaries with different temperatures. If this is true, linear  $\beta$  profiles should be expected not only when  $\beta_L = 1/T_L$  and  $\beta_R = 1/T_R$  are both positive or both negative (a result which could have been deduced from Eq. (2) as well), but also when one of the two baths is kept at positive temperature and the other one at negative temperature. Since this point might appear not obvious in the light of some criticisms moved against the whole concept of negative temperatures [18, 19], it is worth mentioning a simple argument which suggests the linearity of  $\beta$  profiles in conditions close to equilibrium, without making explicit use of the Fourier law.

Let us consider a homogeneous lattice of interacting particles, whose length  $L$  along the  $x$  axis is much larger than the size of any transversal section, so that it can be considered as a one-dimensional system. Particles are not allowed to leave their sites, but they can interact via short-range forces, which allow for heat transfer within the bar. The system is completely isolated, except for the left and right ends, which are subject to the action of external thermal bath, which keep them at inverse temperatures  $\beta_L$  and  $\beta_R$ , respectively. Stationary out-of-equilibrium conditions are realized as soon as  $\beta_R \neq \beta_L$ . Assuming that the total number of sites is very large, we can divide the lattice into  $N \gg 1$  identical cells of linear size  $\Lambda = L/N$ , identified by integer indexes  $n = 1, \dots, N \gg 1$ , each of them still containing a large number of particles. The cell size  $\Lambda$  must be much larger than the typical interaction radius of the particles and the transversal size of the bar. We expect each cell to be found in a state of local equilibrium, described by local thermodynamic variables as the energy  $E_n$  and the entropy  $S(E_n)$ , regarded as a function of the energy of the cell. Notice that  $S$  and  $E_n$  scale with  $\Lambda$ . Let us

consider a pair of consecutive cells  $n$  and  $n + 1$ : their energies  $E_n$  and  $E_{n+1}$  are very close but still different. We want to establish a “degree of local nonequilibrium”  $G_n$  for the considered pair of cells. First we compute the *a priori* probability  $P_n$  of a configuration with the observed energy values  $E_n$  and  $E_{n+1}$ , given the total energy  $2E^{eq} = E_n + E_{n+1}$ . Recalling Boltzmann formula

$$S(E) = \ln W(E) \quad (4)$$

where  $W(E)$  is the number of states accessible to the system at energy  $E$ , we get

$$P_n = \exp[S(E_n) + S(E_{n+1}) - 2S(E^{eq})]. \quad (5)$$

Then we define

$$G_n = -\log(P_n) = 2S(E^{eq}) - S(E_n) - S(E_{n+1}), \quad (6)$$

so that  $G_n$  vanishes when the system is at equilibrium and it increases when the equilibrium probability of the thermodynamic state decreases. By defining

$$\Delta_n = E_n - E^{eq} = E^{eq} - E_{n+1} \quad (7)$$

we can expand Eq. (6) assuming that  $\Delta_n$  is small, so to obtain

$$G_n \simeq -\frac{\partial^2 S}{\partial E_n^2} \Delta_n^2, \quad (8)$$

and we can introduce a corresponding global observable for the whole system as

$$\mathcal{G} = \sum_{n=1}^N G_n. \quad (9)$$

Taking the continuum limit

$$\frac{E_n}{\Lambda} \rightarrow \varepsilon(x) \quad \frac{\partial^2 S}{\partial E_n^2} \Lambda \rightarrow \beta'(\varepsilon(x)) \quad \frac{\Delta}{\Lambda} \rightarrow \frac{1}{2} \varepsilon'(x), \quad (10)$$

where we have exploited the definition of inverse temperature

$$\beta(\varepsilon(x_n)) = \frac{\partial S}{\partial E}, \quad (11)$$

we get

$$\mathcal{G} \rightarrow \frac{1}{4} \int_0^L \beta'(\varepsilon(x)) [\varepsilon'(x)]^2 dx. \quad (12)$$

It is a reasonable physical assumption that the stationary temperature profile of the one-dimensional system will minimize  $\mathcal{G}$ . Indeed, larger values of  $\mathcal{G}$  correspond to less probable configurations. Such minimization can be realized with a variational approach, leading to the Euler-Lagrange equation

$$\frac{\partial^2 \beta}{\partial \varepsilon^2} [\varepsilon'(x)]^2 + 2 \frac{\partial \beta}{\partial \varepsilon} \varepsilon''(x) = 0. \quad (13)$$

Once the function  $\beta(\varepsilon)$  is known, Eq. (13) is a (possibly difficult) second order ordinary differential equation, which only needs to be completed with the conditions  $\beta(\varepsilon(0)) = \beta_L$  and  $\beta(\varepsilon(L)) = \beta_R$  to be solvable.

Let us notice that the system is close to equilibrium, so that  $\varepsilon$  is not expected to vary too much along the lattice and we can exploit the linearization

$$\beta(\varepsilon) = \beta_0 + c\varepsilon, \quad (14)$$

Eq. (13) reduces to the condition  $\varepsilon''(x) = 0$ , so that the energy profile is linear and so is  $\beta(\varepsilon(x))$  (by virtue of condition (14)). This result does not depend on the specific signs of the boundary temperatures. In the specific case where  $\beta_L$  and  $\beta_R$  have the same sign, we can simply recover the linearity of the profile of  $T$ . Indeed

$$\frac{d^2 T}{dx^2} = \frac{2}{\beta^3} \left( \frac{d\beta}{dx} \right)^2 - \frac{1}{\beta^2} \frac{d^2 \beta}{dx^2} \approx \frac{2}{\beta^3} \left( \frac{d\beta}{dx} \right)^2 \quad (15)$$

is a quantity of order  $(\beta_L - \beta_R)^2$ ; when the difference between the inverse temperatures of the baths is small,  $d^2 T/dx^2$  is negligible and the temperature profile is linear, as it would be expected from the empirical Fourier law (2). As expected, this result is not valid anymore when  $\beta(x)$  in the r.h.s. of Eq. (15) vanishes for some  $x$ , a condition which can be realized when  $\beta_L$  and  $\beta_R$  have opposite signs.

As a final remark, we point out that the functional  $\mathcal{G}$  in Eq. (12) is related to the form of the entropy production

$$W = \int_0^L j \beta'(\varepsilon(x)) \varepsilon'(x) dx, \quad (16)$$

once a proportionality relation is established between the heat flux  $j$  and the energy density gradient  $\varepsilon'(x)$ . Accordingly, in this regime, the minimization of  $\mathcal{G}$  corresponds to the well known principle of minimum entropy production [20].

### III. SPIN CHAIN

The first experiments involving equilibrium states at negative temperature were realized by Purcell, Pound and Ramsey, who were studying systems of nuclear spins exposed to intense external field [6, 21]. In this regime interactions are negligible, so that the energy of the system can be written as

$$\mathcal{H}(\boldsymbol{\sigma}) = - \sum_{n=1}^N B \sigma_n \quad (17)$$

where  $\sigma_n = \pm 1$  is the  $n$ -th spin (with  $n = 1, \dots, N$ ,  $N \gg 1$ ) and  $B$  represents the external magnetic field, which is supposed to be homogeneous. If there is a large time-scale separation between the typical thermalization times of the internal dynamics and those needed for a

complete equilibration with the environment, and we focus on intermediate time-scales, the system can be considered both isolated and at equilibrium [21, 22]. Due to energy conservation, only simultaneous flipping of pairs of spins with opposite signs are allowed [23].

Let us denote the number of positive and negative spins by  $N_+$  and  $N_- = N - N_+$ , respectively: in the simple model (17) conservation of energy is equivalent to keeping  $N_+$  (or  $N_-$ ) fixed, so that we can conveniently write an expression for the global entropy as

$$S(N_+) = \ln \left( \frac{N!}{N_+!N_-!} \right) \quad (18)$$

$$\approx -N_+ \ln \left( \frac{N_+}{N} \right) + N_- \ln \left( \frac{N_-}{N} \right) + O(\ln N)$$

where we have exploited Stirling's approximation; the entropy per particle reads therefore

$$s(p) = -p \ln(p) - (1-p) \ln(1-p) \quad (19)$$

where  $p = N_+/N$  is the density of positive spins. Now we can take advantage of the invertible relation between the specific energy  $\varepsilon$  and  $p$ , i.e.

$$\varepsilon = B(1 - 2p), \quad (20)$$

which follows from Eq. (17); we can thus write an explicit expression for  $s(\varepsilon, B)$ :

$$s(\varepsilon, B) = -\frac{B-\varepsilon}{2B} \ln \left( \frac{B-\varepsilon}{2B} \right) - \frac{B+\varepsilon}{2B} \ln \left( \frac{B+\varepsilon}{2B} \right). \quad (21)$$

Taking the derivative of the above equation with respect to  $\varepsilon$ , for a fixed value of the external field, we get the inverse (microcanonical) temperature:

$$\beta(\varepsilon, B) = \frac{\partial s}{\partial \varepsilon} = \frac{1}{2B} \ln \left( \frac{B-\varepsilon}{B+\varepsilon} \right). \quad (22)$$

The specific energy  $\varepsilon$  ranges from  $-B$  to  $B$ , corresponding to the extreme cases in which all spins are positive or negative, respectively. As a consequence, the value of  $\beta$  ranges from  $-\infty$  to  $+\infty$ . Negative temperatures correspond to positive-energy cases in which most spins are not aligned with the external magnetic field. Let us also notice that by substituting Eq. (20) into Eq. (22) and inverting, one finds

$$p = \frac{e^{\beta B}}{2 \cosh(\beta B)}, \quad (23)$$

which is consistent with the statistical interpretation of  $p$  as the probability that a given spin is positive, once the inverse temperature  $\beta$  of the system is known. Similarly, the magnetization density of the system,  $m = (N_+ - N_-)/N$ , verifies

$$m = 2p - 1 = \tanh(\beta B). \quad (24)$$

So far we have just recalled known equilibrium results for systems of Ising spins subjected to a strong external field. In the following we will consider a linear geometry, i.e. we will assume that the spins are placed on the sites of a one-dimensional lattice. Taking into account local conservation of energy, we impose that only pairs of (opposite) spins located on *neighbour* sites can exchange energy by simultaneous flipping. In particular, we model the dynamics assuming that at regular time intervals one of the  $2(N-1)$  *ordered* pairs of neighbour spins is randomly chosen (i.e., the couples  $(n, n+1)$  and  $(n+1, n)$  are regarded as different choices): if the first spin of the pair is positive and the second is negative, they both flip; otherwise, nothing happens. We will also consider thermal baths on the boundary sites of the chain, characterized by inverse temperatures  $\beta_L$  and  $\beta_R$ . If  $\beta_R \neq \beta_L$  the system is out of equilibrium, and we can ask what is the shape of the temperature profile in this case. Notice that, in principle, one or both thermal baths can be characterized by negative temperature.

If the system reaches a stationary state, local conservation of energy implies that the average energy flux must be constant along the lattice. The dynamics can be conveniently mapped into an exclusion process [24], in which all positive spins are replaced by particles and all negative spins by empty sites; particles can only move to a neighbour site if this is empty, and each particle carries an amount of energy equal to  $-2B$ . With this scheme in mind, the average energy flux between the  $n$ -th and  $(n+1)$ -th site is given by

$$\langle j_n \rangle = -2B (p_n w_{n \rightarrow n+1} - p_{n+1} w_{n+1 \rightarrow n}), \quad (25)$$

where  $p_n$  is the probability of finding a particle in the  $n$ -th site (or, equivalently, the average occupation number of the  $n$ -th site), while  $w_{n \rightarrow k}$  is the transition rate from site  $n$  to site  $k$ . The latter can be written in terms of the occupation probability as

$$w_{n \rightarrow k} = \frac{1}{\tau} \text{Prob}(k \text{ empty} \mid n \text{ occupied}) \approx \frac{1-p_k}{\tau}, \quad (26)$$

where  $\tau$  is the average time interval between two consecutive extractions of the ordered pair  $(n, k)$ . Indeed, in our model, once the pair has been extracted, the transition only happens if site  $k$  is empty. In the above equation we have assumed that the probability of finding a particle in the  $k$ -th site does not depend on the occupation of its neighbour site  $n$ : this simplifying hypothesis, somehow resembling Boltzmann's "molecular chaos" assumption, is actually not true, since the dynamics may induce correlations between the occupation numbers of neighbour sites; however we can reasonably expect such correlations to be negligible in typical conditions. The condition that  $\langle j_n \rangle$  assumes the same value for each  $n$  in the stationary state (i.e.  $\langle j_n \rangle \equiv j \forall n$ ) leads then to

$$p_n(1-p_{n+1}) - p_{n+1}(1-p_n) = p_n - p_{n+1} = \text{const.} \quad (27)$$

As a consequence, the nonequilibrium occupation proba-

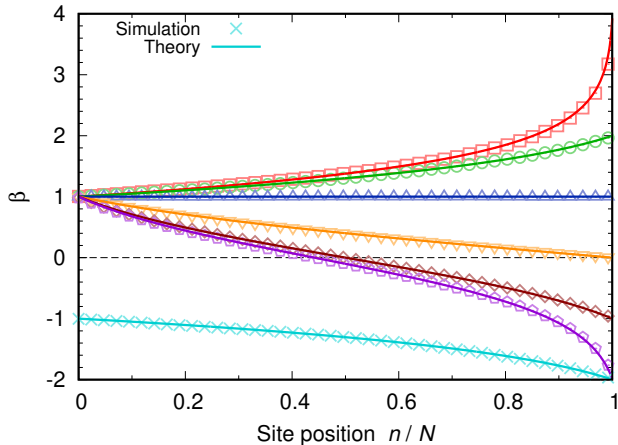


Figure 1. Inverse temperature profiles for the spin chain, for different choices of the boundary conditions. Points are obtained by measuring the local inverse temperature, solid lines are computed assuming that Eq. (28) holds. Parameters:  $\tau'/\tau = 1$ ,  $h = 1$ ,  $N = 128$ .

bility of the  $n$ -th site reads

$$p_n = p_L + \frac{n-1}{N-1}(p_R - p_L) \quad (28)$$

where  $p_L$  and  $p_R$  are the average occupation numbers of the leftmost ( $n = 1$ ) and rightmost ( $n = N$ ) sites, fixed by the boundary conditions. Assuming local equilibrium, we can expect  $p_n$  to be well described by Eq. (23) for the density of positive spins, where  $\beta$  has now the meaning of a local inverse temperature. The relation can be inverted numerically so to find the  $\beta$  profile along the lattice.

We can compare the above discussed results with the outcomes of numerical simulations in out-of-equilibrium conditions. The action of the thermal baths at the boundaries is mimicked by imposing that the probabilities  $p_L$  and  $p_R$  of a positive value of the leftmost and rightmost spin, respectively, are given by

$$p_{L,R} = \frac{e^{\beta_{L,R}B}}{2 \cosh(\beta_{L,R}B)}. \quad (29)$$

In this simple case, to impose the above distribution it is sufficient to update from time to time the extremal spins, extracting their values according to the above probabilities. The time intervals between consecutive updates are determined by a Poisson process with characteristic time  $\tau'$ . We can then determine the local inverse temperature by measuring the local magnetization density and inverting relation (24). It can be verified that, if  $\tau'/\tau \leq 1$ , the external baths are able to keep the temperatures of the extremal sites fixed. The temperature profiles for various choices of  $\beta_L$  and  $\beta_R$  are shown in Figure 1, where the theoretical expectations are also plotted.

Let us remark that the presence of negative values of  $\beta_R$  and/or  $\beta_L$  does not hinder the possibility to reach a stationary state, characterized by constant energy flux

along the chain; this is a first, simple example of Fourier-like transport in negative-temperature conditions. We also notice that, consistently with the discussion in Section II, the inverse temperature profile is continuous when passing from positive to negative values; the temperature profile would show instead a singularity when  $\beta = 0$ .

We can also measure the “conductivity”  $\gamma$  introduced in Eq. (3), which, at variance with  $\kappa$ , is well defined even when the boundaries of the chain are found at temperatures with different signs. To this end, from Eqs. (25) and (26) we can derive an explicit expression for the average value of the “total” heat flux

$$J = \sum_{n=1}^N j_n, \quad (30)$$

namely

$$\langle J \rangle = \frac{2B}{\tau}(p_R - p_L). \quad (31)$$

By using Eq. (23) and expanding to the linear order in  $\Delta\beta = \beta_R - \beta_L$ , we obtain

$$\langle J \rangle \simeq \frac{1}{\tau} \left( \frac{B}{\cosh(\beta B)} \right)^2 \Delta\beta + O(\Delta\beta^2). \quad (32)$$

Accordingly,

$$\gamma = \lim_{\Delta\beta \rightarrow 0} \frac{J}{\Delta\beta} = \frac{1}{\tau} \left( \frac{B}{\cosh(\beta B)} \right)^2. \quad (33)$$

In Fig. 2 we compare the measured values of  $\gamma$  obtained from numerical simulations with the analytical expression Eq. (33). The reported plots show a nice agreement for different values of the “operating” temperature  $\beta$ , also in the negative-temperature region. Interestingly, the condition of maximal conductivity is obtained precisely at  $\beta = 0$ , i.e. when the two thermal baths operate at opposite inverse temperatures.

#### IV. HAMILTONIAN COUPLED ROTATORS

Negative temperature can be also found in Hamiltonian chains of the form

$$\mathcal{H}(\mathbf{p}, \mathbf{q}) = \sum_{n=1}^N \mathcal{K}(p_n) + \sum_{n=1}^{N-1} \mathcal{U}(q_{n+1} - q_n). \quad (34)$$

where the canonical variables  $\{q_n, p_n\}$  live in a  $2N$ -dimensional bounded phase space, while  $\mathcal{K}(p_n)$  represents a generalized kinetic term and  $\mathcal{U}(q_{n+1} - q_n)$  is some interaction potential. In the following we will specialize to the case

$$\mathcal{H}(\mathbf{p}, \mathbf{q}) = \sum_{n=1}^N (1 - \cos p_n) + \varepsilon \sum_{n=1}^{N-1} [1 - \cos(q_{n+1} - q_n)], \quad (35)$$

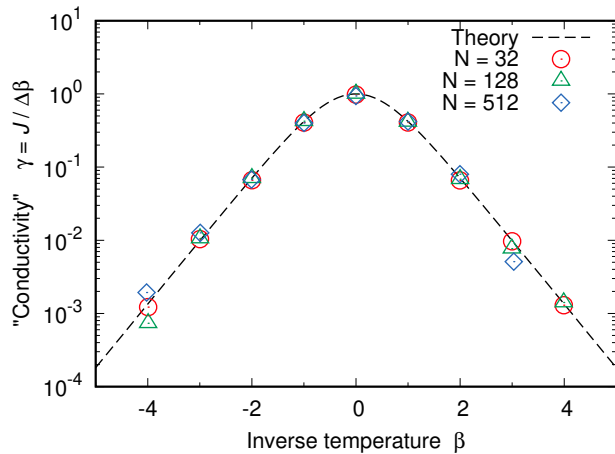


Figure 2. Conductibility of the spin chain as a function of the inverse temperature  $\beta$ . Points are obtained by measuring the energy flux along spin chains whose boundaries are kept at fixed inverse temperature  $\beta \pm 0.05$ , for three different values of  $N$ . The dashed line refers to the theoretical prediction (33). Parameters:  $\tau'/\tau = 1$ ,  $B = 1$ .

i.e. a chain of  $N$  particles characterized by kinetic terms which are periodic in the momenta, and potential interactions typical of systems of classical rotators [25, 26]. The phase space  $[0, 2\pi)^{2N}$  of the coordinate variables is bounded, and this allows for the occurrence of negative temperature states. The equilibrium properties of models of this kind have been investigated in previous works [13–15]. Here we are interested in transport phenomena due to the presence of a temperature gradient. To this end, as in the case of the spin chain discussed previously, we need to impose different values  $\beta_L$  and  $\beta_R$  of the inverse temperature at the boundaries (particles labeled by  $n = 1$  and  $n = N$ ), by means of suitable stochastic heat baths. The most natural way to impose an equilibrium distribution on the  $n$ -th particle is to implement a dynamics ruled by the *generalized* Klein-Kramers equation

$$\begin{pmatrix} \dot{q}_n \\ \dot{p}_n \end{pmatrix} = \begin{pmatrix} \partial_{p_n} \mathcal{K} \\ -\partial_{q_n} \mathcal{H} - D_n \beta_i \partial_{p_n} \mathcal{K} + \sqrt{2D_n} \xi(t) \end{pmatrix}, \quad (36)$$

where  $\xi(t)$  represents a Gaussian delta-correlated noise and  $D$  is a parameter determining a typical frequency for the thermal bath. It can be shown that this stochastic differential equation reproduces the effect of an actual mechanical bath composed by a large number of particles with smaller inertia [15]. A similar equation also holds if the bath is composed by a set of Ising spins ruled by a Glauber dynamics and interacting with the considered particle [27].

We implement molecular dynamics simulations using the algorithm discussed in Ref. [28]; this integration scheme is quasi-symplectic, meaning that it exactly reduces to a symplectic algorithm (second-order Verlet) in the limit of vanishing noise [29]. The integration step  $\Delta t$  is chosen by imposing that, in the zero-noise limit, the

value of total energy is conserved, with relative fluctuations of order  $\simeq 10^{-5}$ . Determining the optimal value for  $D$  is a slightly less trivial task, since it is known that the actual effect of Langevin-like baths in Hamiltonian one-dimensional chains is related to the characteristic time scale of the stochastic dynamics [2]. This problem is discussed in Appendix A in some detail.

We start our analysis by focusing on heat transport at positive temperatures. A consistency check for our setup can be done by measuring the thermal conductivity

$$\kappa = \frac{Nj}{\beta_L^{-1} - \beta_R^{-1}}, \quad (37)$$

where  $j$  is the local value of the heat flux, which can be identified with a suitable mechanical observable following the discussion in Ref. [2]; first, we define the local energy as

$$h_n = \mathcal{K}_n(p_n) + \frac{1}{2} [\mathcal{U}_n(q_{n+1} - q_n) + \mathcal{U}_{n-1}(q_n - q_{n-1})], \quad (38)$$

and we consider its time derivative

$$\begin{aligned} \dot{h}_n &= \frac{1}{2} \mathcal{U}'_n(q_{n+1} - q_n) [\mathcal{K}'_{n+1}(p_{n+1}) + \mathcal{K}'_n(p_n)] + \\ &\quad - \frac{1}{2} \mathcal{U}'_{n-1}(q_n - q_{n-1}) [\mathcal{K}'_n(p_n) + \mathcal{K}'_{n-1}(p_{n-1})]. \end{aligned} \quad (39)$$

The above expression has to be compared with the definition of heat flux in a linear lattice

$$\dot{h}_n + j_n - j_{n-1} = 0, \quad (40)$$

where a unitary distance between neighbour sites on the lattice is assumed. We can thus identify the local heat flux as

$$j_n = -\frac{1}{2} \mathcal{U}'_n(q_{n+1} - q_n) [\mathcal{K}'_n(p_n) + \mathcal{K}'_{n+1}(p_{n+1})], \quad (41)$$

which in our case specializes into

$$j_n = -\frac{\varepsilon}{2} \sin(q_{n+1} - q_n) [\sin p_n + \sin p_{n+1}]. \quad (42)$$

In the stationary state,  $j = \langle j_n \rangle$  is expected to be independent of the site  $n$ .

If the difference between the temperatures of the thermal baths is small, the total heat flux

$$J = \sum_{n=1}^N j_n \quad (43)$$

can be seen as the stationary response to a perturbation of the equilibrium distribution function, and a Green-Kubo relation between the conductivity and the auto-correlation of  $J$  can be found [2, 30]:

$$\frac{\kappa_{GK}}{\beta^2} = \lim_{t \rightarrow \infty} \int_0^t d\tau \lim_{N \rightarrow \infty} \frac{\langle J(\tau) J(0) \rangle}{N}. \quad (44)$$

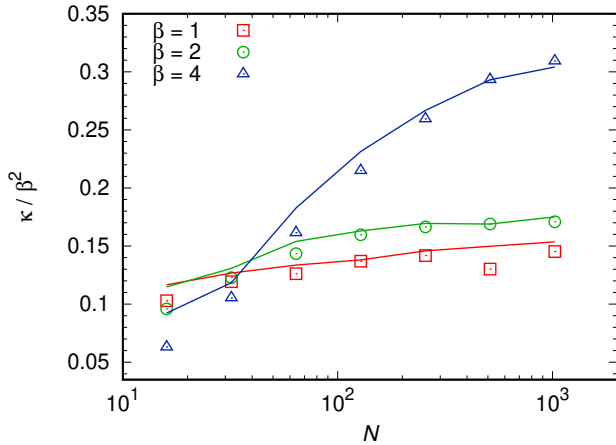


Figure 3. Size-dependence of thermal conductivity for the rotators model (35). For different values of  $\beta$ , the results of out-of-equilibrium numerical simulations in which  $\beta_{L,R} = (1 \pm 0.05)\beta$  are shown. Points represent conductivity  $\kappa$  as measured in numerical simulations from its definition (37); solid lines are computed according to the right hand side of Eq. (44) at finite  $N$ . Here  $D = 0.4$ ; other parameters as in Fig. 8.

In Fig. 3 we compare the values of  $\kappa$  measured in numerical simulations to the prediction  $\kappa_{GK}$  based on the Green-Kubo analysis, for fixed size of the chain (i.e., we do not take the  $N \rightarrow \infty$  limit) in conditions close to thermal equilibrium. Let us notice, incidentally, that only for  $\beta$  small enough the conductivity reaches a finite limit at large  $N$  (normal conduction) – or, at least, the value of  $N$  at which  $\kappa$  reaches a plateau seems to depend on the inverse temperature. This is consistent with known results for the case of classical rotators (characterized by the same potential terms as in Eq. (35), but usual quadratic kinetic terms): in that case a transition between two regimes of transport is observed for  $\beta \simeq 3$  [26].

Finally, in Fig. 4 we plot the local inverse temperature  $\beta_n$  of the chain, as a function of the site  $n$ , for different values of  $\beta_L$  and  $\beta_R$ . Here  $\beta_n$  is measured by inverting the relation

$$\langle \cos p_n \rangle = \frac{\int_0^{2\pi} dp_n e^{-\beta_n \mathcal{K}(p_n)} \cos p_n}{\int_0^{2\pi} dp_n e^{-\beta_n \mathcal{K}(p_n)}} = \frac{I_1(\beta_n)}{I_0(\beta_n)}, \quad (45)$$

$I_n(x)$  being the modified Bessel function of the first kind. The inverse temperature profile does not significantly deviate from the linear behaviour predicted by the simple argument in Section II. Let us stress once again that this is also true when one or both temperatures are negative; as a consequence, the crossing between the positive- and negative-temperature regime occurs at  $\beta = 0$ , suggesting once again that this state is physically meaningful and may be realized in out-of-equilibrium chains allowing for negative temperature states.

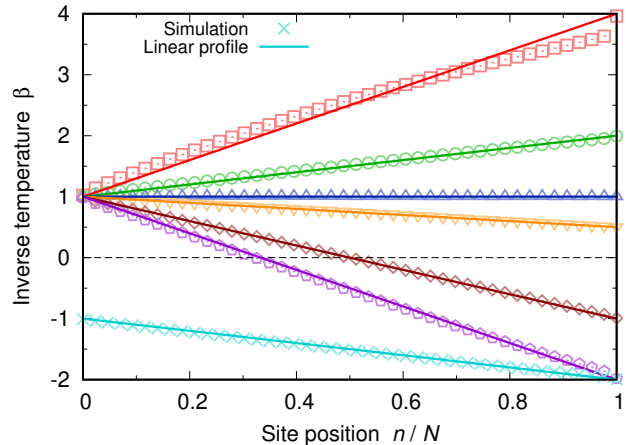


Figure 4. Inverse temperature profiles for system (35) driven out of equilibrium. Points represent the outcomes of numerical simulations, solid lines the linear profile between the considered inverse temperatures. Parameters:  $\varepsilon = 0.5$ ,  $N = 1024$ ,  $D = 0.4$ ,  $\Delta t = 3 \cdot 10^{-2}$ .

## V. LINEAR-STOCHASTIC SCHRÖDINGER EQUATION

Fourier transport at negative temperatures may arise even in more complex setups as those involving coupled transport, i.e. when two or more species of currents flow through the system and influence one another [31]. The study of coupled transport phenomena in chains of coupled oscillators is a relatively recent topic [24, 32–36] In this section we will focus on a minimalist model of a chain of coupled Schrödinger oscillators defined by the equations

$$i\dot{z}_n = -z_{n+1} - z_{n-1} \quad n = 1, \dots, N \quad (46)$$

where the variables  $z_n$  and  $iz_n^*$  are a couple of complex-valued canonical variables for the Hamiltonian

$$H = \sum_{n=1}^N z_n^* z_{n+1} + z_n z_{n+1}^* \quad (47)$$

and open boundary conditions  $z_0 = z_{N+1} = 0$  are assumed. This model can be regarded as the linear limit of the celebrated Discrete Nonlinear Schrödinger equation [37]. Given its linear structure, the model can be exactly diagonalized, giving rise to  $(N - 1)$  additional conserved quantities besides energy. Among them, the conservation of the total norm

$$A = \sum_{n=1}^N |z_n|^2 \quad (48)$$

is related to the invariance of Eq. (46) under global phase transformations of the  $z_n$  in the complex plane.

While the dynamics of Eq. 46 is completely integrable and gives rise naturally to ballistic transport, in [16] it was shown that in the presence of a suitable external conservative noise, the set of conserved quantities can be reduced to the couple  $(A, H)$ . The irreversible dynamics amounts to the addition of conservative “collisions” among neighbouring oscillators occurring at rate  $\nu_c$ . Such collisions can account, for example, for the effect of a weak nonlinearity of the equations of motion [38]. In detail, given a randomly selected site  $n = 2, \dots, N - 1$  in the bulk of the chain, a collision event consists in modifying the phase  $\phi_n = \arg(z_n)$  such that the local energy density  $h_n = (z_n^* z_{n+1} + z_n^* z_{n-1} + c.c.)/2$  is conserved. In addition, this pure phase transformation conserves the local norm  $|z_n|^2$  and therefore  $A$ . Collision events occur at random times, whose separations  $\tau$  are independent and identically distributed random variables extracted from a Poissonian distribution  $P(\tau) \simeq \exp(-\nu_c \tau)$ . Given its mixed linear-deterministic and stochastic evolution, we will refer to the model as the Linear-Stochastic Schrödinger (LSS) equation.

The equilibrium properties of the LLS model were discussed in [16, 39] within the grand-canonical ensemble and they can be summarized in the phase diagram shown in Fig. 5, which involves the norm density  $a = A/N$  and the energy density  $h = H/N$ . The solid black and purple lines, defined by  $h = \mp 2a$ , represent respectively the ground state ( $\beta = +\infty$ ) and the maximum energy state ( $\beta = -\infty$ ), while the horizontal dot-dashed line is the  $\beta = 0$  isothermal. The region of parameters above this line is characterized by negative absolute temperatures, see orange area. Equilibrium states at positive temperatures lie below the  $\beta = 0$  line, see turquoise region.

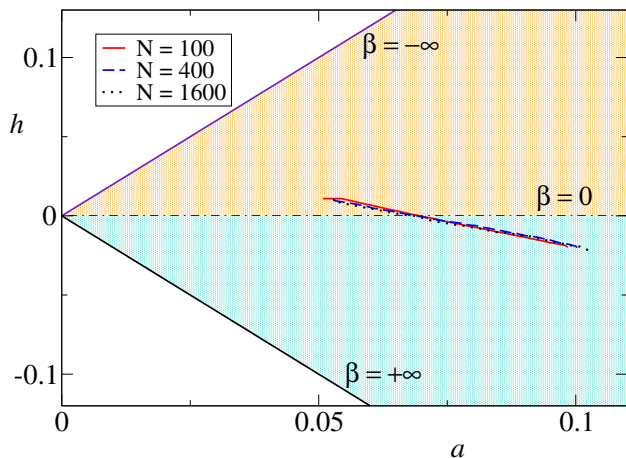


Figure 5. Thermodynamic diagram  $(a, h)$  of the LSS equation. Black and purple solid lines are, respectively, the ground state ( $\beta = +\infty$ ) and the  $\beta = -\infty$  state. The horizontal dot-dashed curve identifies the  $\beta = 0$  line. Parametric plots  $[a(x), h(x)]$  of nonequilibrium density profiles are shown for  $\beta_L = -2$ ,  $\beta_R = 1$ ,  $\mu_L = 10$  and  $\mu_R = -10$ .

The transport properties of the model were studied in [16] within the positive temperature region. In par-

ticular, it was found that transport is diffusive and that the Seebeck coefficient is non-vanishing, thus revealing the existence of coupled-transport [40]. In the following we will show that the above model displays Fourier transport also at negative temperatures.

The study of the nonequilibrium problem can be accomplished by imposing suitable imbalances of inverse temperature  $\beta_R - \beta_L$  and of chemical potential  $\mu_R - \mu_L$  at the boundaries of the chain. To this end, we will consider the following Langevin equation specified for the left reservoir connected to the lattice site  $n = 1$

$$i\dot{z}_1 = -(1 + i\alpha_L)z_2 + i\alpha_L\mu_L + \sqrt{\alpha_L/\beta_L}\eta(t), \quad (49)$$

where  $\alpha_L$  specifies the coupling parameter and  $\eta(t)$  is a (complex) Gaussian white noise with zero mean and unit variance satisfying  $\langle \eta(t)\eta(t') \rangle = \delta(t - t')$ . An analogous equation holds for the right reservoir acting on site  $n = N$  and characterized by parameters  $\alpha_R, \beta_R, \mu_R$ . The derivation of Eq. (49) is discussed in [41] assuming that  $\beta_L$  and  $\alpha_L$  are both positive-definite. In analogy with [15] it can be formally extended to the case  $\beta_L < 0$  by requiring  $\alpha_L < 0$ , thus replacing the standard dissipative term with a gain.

In addition to the boundary thermodynamic parameters, one needs to perform measurements of inverse temperature and chemical potential profiles. This task is accomplished for the LSS equation by making use of suitable microcanonical observables derived from the thermodynamic relations  $\beta = \partial\mathcal{S}/\partial E|_{A=M}$  and  $-\beta\mu = \partial\mathcal{S}/\partial A|_{H=E}$ , for a system with total energy  $H = E$ , total norm  $A = M$  and entropy  $\mathcal{S}$ , see [32, 42] for details.

In Fig. 6 we show nonequilibrium stationary profiles corresponding to a LSS equation in contact with boundary reservoirs with inverse temperature  $\beta_L = -2$  and  $\beta_R = 1$  with chemical potentials  $\mu_L = 10$  and  $\mu_R = -10$ . We have chosen  $\nu_c = 1$ ,  $\alpha_L = -1$  and  $\alpha_R = 1$ . All profiles display an extensive scaling for different system sizes  $N$  and they nicely overlap once reported as a function of the intensive spatial variable  $x = n/N$ . As discussed for the previous models, the profiles of  $\beta(x)$  cross smoothly the  $\beta = 0$  point (panel (a)). The same is observed for the profiles of  $(\beta\mu)(x)$  (panel (b)), where such a crossing occurs for a finite value of  $\beta\mu$ . This is consistent with the fact that on the  $\beta = 0$  line in Fig. 5 the chemical potential has a discontinuity  $\mu = \pm\infty$ . Therefore, it appears that the second appropriate thermodynamic variable (besides  $\beta$ ) to describe coupled transport across  $\beta = 0$  is  $\beta\mu$ . The corresponding profiles of local energy  $h(x)$  and norm  $a(x)$  are shown in panels (c) and (d), respectively.

The same density profiles are represented parametrically in the diagram  $(a, h)$  in Fig. 5, where they correspond to overlapping linear lines that connect the regions of positive and negative temperatures.

To better analyze the properties of the transport process, we have measured the stationary currents of norm and energy, which are respectively defined [16, 32] as

$$\dot{j}_a = 2\langle \text{Im}(z_n^* z_{n+1}) \rangle, \quad \dot{j}_h = 2\langle \text{Re}(\dot{z}_n z_{n+1}^*) \rangle, \quad (50)$$

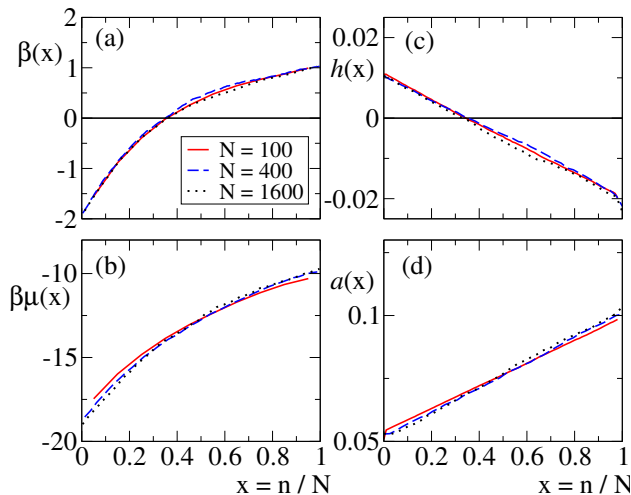


Figure 6. Nonequilibrium stationary profiles a LSS chain of  $N = 100, 400$  and  $1600$  sites and parameters  $\beta_L = -2$ ,  $\beta_R = 1$ ,  $\mu_L = 10$  and  $\mu_R = -10$ . Simulations are obtained evolving the LSS system for  $5 \cdot 10^6$  time units after a transient of  $10^6$  time units with parameters  $\nu_c = 1$ ,  $\alpha_L = -1$  and  $\alpha_R = 1$ .

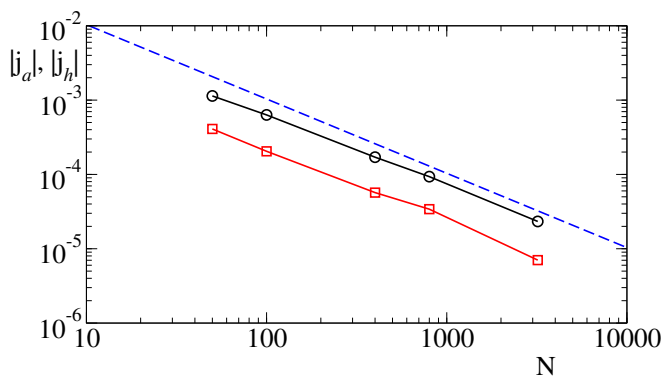


Figure 7. Average norm flux (black circles) and energy flux (red squares) versus chain size  $N$  for a LSS system with  $\beta_L = -2$ ,  $\beta_R = 1$ ,  $\mu_L = 10$  and  $\mu_R = -10$ . The blue dashed line shows the scaling  $1/N$ .

where the symbol  $\langle \cdot \rangle$  represents the average over the nonequilibrium stationary distribution. These currents are reported (in absolute value) in Fig. 7 as a function of the system size  $N$ . A clear dependence as  $1/N$  is observed for both currents, thus confirming that Fourier coupled transport is established.

## VI. CONCLUSIONS

We have presented a study of thermal transport in one-dimensional models compatible with negative absolute temperatures and we have performed a first exploration of their stationary states in the negative temperature region. We have considered three different types of microscopic dynamical evolution, namely a purely stochastic

spin chain, a deterministic Hamiltonian model of rotators and a mixed deterministic-stochastic model of complex coupled oscillators. While the first two models are characterized by transport of a single (heat) current, the third one admits two independent currents, hence coupled transport in the sense of irreversible thermodynamics.

The necessity to impose given values of the thermodynamic parameters at the chain ends requires the introduction of external reservoirs working both at positive and negative temperatures. Such reservoirs have been implemented in the spin chain by simply imposing the target equilibrium distribution on the extremal spins, and in the oscillators model as a Langevin equation complementing the deterministic dynamics.

We have shown that the natural thermodynamic parameters for the description of negative-temperature transport are the inverse temperature  $\beta$  and, when coupled transport is present, the quantity  $\beta\mu$ . Within this representation, no intrinsic singularities occur upon crossing the infinite-temperature ( $\beta = 0$ ) point. Indeed, our results show that stationary transport regimes connecting the positive- and negative-temperature regions are physically accessible. In this generalized transport setup, a form of the Fourier law as in (3) describes consistently diffusive transport through the conductivity parameter  $\gamma$ , see also Eq. (33) in the whole space of accessible thermodynamic parameters. We remark that for the models here considered,  $\gamma$  turns out to be finite in the limit of large system sizes  $N$ , i.e. transport is normal.

Among the possible perspectives, a natural one is to identify and study further models of negative-temperature transport. This task is less obvious than one can imagine. Indeed, beyond the identification of a model where negative temperatures are accessible, one has to verify that the coupling with external reservoirs at negative temperatures is compatible with the physics of the system. A relevant example where this program breaks down is the Discrete Nonlinear Schrödinger equation [37]. Recent studies have shown that this system displays negative temperature states only within the microcanonical ensemble, while a grand-canonical description is forbidden because of nonequivalence of statistical ensembles [43]. As a result, the system can not be consistently driven to the negative-temperature region by means of a negative-temperature reservoir. On the one hand, this does not exclude the occurrence of negative-temperature transport by large imbalances of positive-temperature reservoirs, as shown in [11]. On the other hand, the joint observation of strongly inhomogeneous profiles appears to forbid any description of the process in terms of generalized conductivity coefficients.

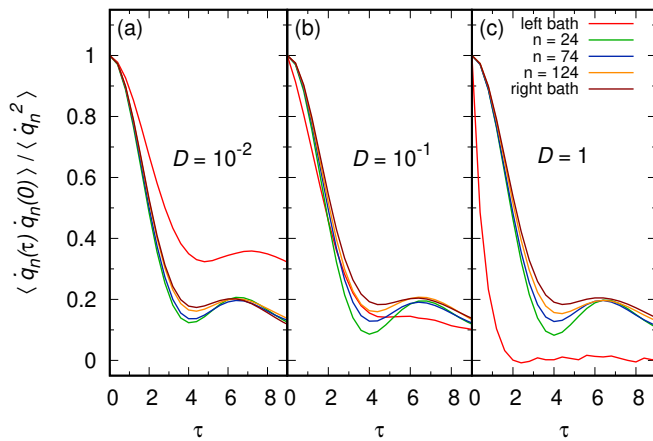


Figure 8. Autocorrelation functions of the rotators model (35) for some particle velocities. Cases  $D = 10^{-2}$ ,  $D = 10^{-1}$  and  $D = 1$  (panels (a), (b) and (c), respectively), are considered: only for the second choice the characteristic times of the boundary particles (subjected to the action of the baths) are comparable with those of the bulk. Parameters:  $\varepsilon = 0.5$ ,  $N = 128$ , integration step  $\Delta t = 3 \cdot 10^{-2}$ .

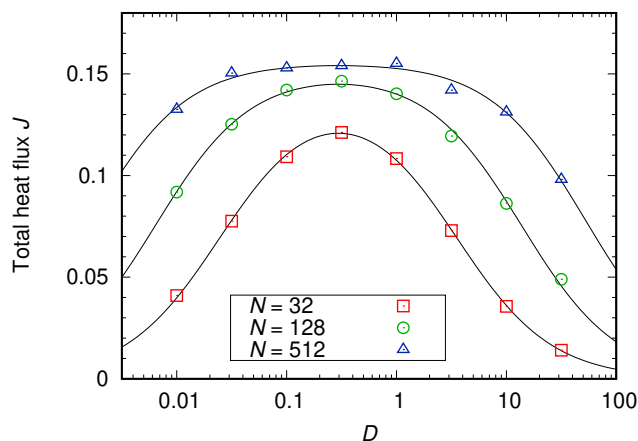


Figure 9. Dependence on  $D$  of the total heat flux of the rotators model (35). For 3 values of  $N$ , the behaviour of  $J$  as a function of  $D$  is shown (points). Black solid lines are obtained with a least-square fit of the heuristic functional form (A1). Here,  $\beta_L = 1$ ,  $\beta_R = 2$ . Other parameters as in Fig. 8.

### Appendix A: Remarks on Langevin-like stochastic baths

In this Appendix we study the problem of finding the optimal value for the parameter  $D$  which characterizes the

thermal baths in Eq. (36). When Langevin-like reservoirs are employed in numerical simulations, fixing the value of the parameters appearing in the stochastic differential equations amounts to determine a typical time scale for their dynamics. If one aims to understand the equilibrium properties of a given system, this fact can be regarded as a secondary aspect, since equilibrium averages are not expected to depend on such dynamical properties. The scenario is different when out-of-equilibrium conditions are considered, since one also needs that the chosen parameters actually reproduce the right dynamics.

For the case of the Hamiltonian rotator model (35), some insight on the best choice for  $D$  can be gained by looking at the autocorrelation functions of some particles for different choices of the parameters, as shown in Fig. 8: for too large (or too small) values of  $D$  the characteristic times of the bulk can be very different from those of the boundary particles, a clear hint that the stochastic dynamics does not reproduce the typical behaviour of the Hamiltonian particles in this case; better agreement is found for  $D \simeq 10^{-1}$ .

A more quantitative analysis can be drawn by studying the behaviour of the heat flux (43). The behaviour of  $J$  as a function of  $D$  is shown in Fig. 9 for some values of  $N$ ; it is nicely fitted by the empirical formula

$$J \approx \frac{c_1 D}{1 + c_2 D + c_3 D^2}, \quad (\text{A1})$$

resembling the one discussed in [2]. When  $N$  large enough, a plateau is observed for values of  $D$  between 0.1 and 1, which maximize the heat flux. For our numerical simulations we chose values of  $D$  in such interval.

### ACKNOWLEDGMENTS

We acknowledge useful discussions with Roberto Livi and Angelo Vulpiani. We thank Stefano Lepri for a critical reading of the manuscript. M. B. acknowledges financial support of MIUR-PRIN2017 *Coarse-grained description for non-equilibrium systems and transport phenomena (CO-NEST)*.

[1] B. Derrida, Physics Reports **301**, 65 (1998).

[2] S. Lepri, R. Livi, and A. Politi, Phys. Rep. **377**, 1

(2003).

[3] M. Pino, L. B. Ioffe, and B. L. Altshuler, Proceedings of

- the National Academy of Sciences **113**, 536 (2016).
- [4] S. Lepri, *Thermal transport in low dimensions: from statistical physics to nanoscale heat transfer*, Vol. 921 (Springer, 2016).
- [5] L. Onsager, *Il Nuovo Cimento (1943-1954)* **6**, 279 (1949).
- [6] N. F. Ramsey, *Phys. Rev.* **103**, 20 (1956).
- [7] A. Oja and O. Lounasmaa, *Rev. Mod. Phys.* **69**, 1 (1997).
- [8] Y. Yatsuyanagi, Y. Kiwamoto, H. Tomita, M. M. Sano, T. Yoshida, and T. Ebisuzaki, *Phys. Rev. Lett.* **94**, 054502 (2005).
- [9] R. Pakter and Y. Levin, *Physical review letters* **121**, 020602 (2018).
- [10] S. Braun, J. P. Ronzheimer, M. Schreiber, S. S. Hodgman, T. Rom, I. Bloch, and U. Schneider, *Science* **339**, 52 (2013).
- [11] S. Iubini, S. Lepri, R. Livi, G.-L. Oppo, and A. Politi, *Entropy* **19**, 445 (2017).
- [12] S. Flach and A. V. Gorbach, *Physics Reports* **467**, 1 (2008).
- [13] L. Cerino, A. Puglisi, and A. Vulpiani, *J. Stat. Mech.* **2015**, P12002 (2015).
- [14] M. Baldovin, A. Puglisi, A. Sarracino, and A. Vulpiani, *J. Stat. Mech.* **2017**, 113202 (2017).
- [15] M. Baldovin, A. Puglisi, and A. Vulpiani, *J. Stat. Mech.* **2018**, 043207 (2018).
- [16] S. Iubini, *Journal of Statistical Mechanics: Theory and Experiment* **2019**, 094016 (2019).
- [17] A. Dhar, *Advances in Physics* **57**, 457 (2008), <https://doi.org/10.1080/00018730802538522>.
- [18] V. Romero-Rochín, *Phys. Rev. E* **88**, 022144 (2013).
- [19] J. Dunkel and S. Hilbert, *Nature Physics* **10**, 67 (2014).
- [20] M. J. Klein and P. H. Meijer, *Physical Review* **96**, 250 (1954).
- [21] E. M. Purcell and R. V. Pound, *Phys. Rev.* **81**, 279 (1951).
- [22] R. V. Pound, *Phys. Rev.* **81**, 156 (1951).
- [23] A. Abragam and W. G. Proctor, *Phys. Rev.* **109**, 1441 (1958).
- [24] S. Iubini, A. Politi, and P. Politi, *J. Stat. Phys.* **154**, 1057 (2014).
- [25] C. Giardinà, R. Livi, A. Politi, and M. Vassalli, *Phys. Rev. Lett.* **84**, 2144 (2000).
- [26] O. V. Gendelman and A. V. Savin, *Phys. Rev. Lett.* **84**, 2381 (2000).
- [27] M. Baldovin, A. Vulpiani, A. Puglisi, and A. Prados, *Phys. Rev. E* **99**, 060101(R) (2019).
- [28] F. Miceli, M. Baldovin, and A. Vulpiani, *Phys. Rev. E* **99**, 042152 (2019).
- [29] S. Melchionna, *J. Chem. Phys.* **127**, 044108 (2007).
- [30] R. Kubo, *Reports on Progress in Physics* **29**, 255 (1966).
- [31] R. Livi and P. Politi, *Nonequilibrium statistical physics: a modern perspective* (Cambridge University Press, 2017).
- [32] S. Iubini, S. Lepri, and A. Politi, *Phys. Rev. E* **86**, 011108 (2012).
- [33] S. Borlenghi, S. Iubini, S. Lepri, J. Chico, L. Bergqvist, A. Delin, and J. Fransson, *Physical Review E* **92**, 012116 (2015).
- [34] S. Iubini, S. Lepri, R. Livi, and A. Politi, *New J. Phys.* **18**, 083023 (2016).
- [35] J. Wang, G. Casati, and G. Benenti, *Physical Review Letters* **124**, 110607 (2020).
- [36] A. Iacobucci, S. Olla, and G. Stoltz, *arXiv preprint arXiv:2006.10431* (2020).
- [37] P. G. Kevrekidis, *The discrete nonlinear Schrödinger equation: mathematical analysis, numerical computations and physical perspectives*, Vol. 232 (Springer Science & Business Media, 2009).
- [38] M. Onorato, G. Dematteis, D. Proment, A. Pezzi, M. Ballarin, and L. Rondoni, *arXiv preprint arXiv:2012.10618* (2020).
- [39] P. Buonsante, R. Franzosi, and A. Smerzi, *Ann. Phys. (N. Y.)* **375**, 414 (2016).
- [40] In the context of linear response theory, the Seebeck coefficient  $S$  corresponds to minus the ratio between the chemical potential gradient and the temperature gradient in the absence of norm flux, see [32] for details. Coupled transport is identified by the condition  $S \neq 0$ .
- [41] S. Iubini, S. Lepri, R. Livi, and A. Politi, *J. Stat. Mech.* **2013**, 08017 (2013).
- [42] R. Franzosi, *Journal of Statistical Physics* **143**, 824 (2011).
- [43] G. Gradenigo, S. Iubini, R. Livi, and S. N. Majumdar, *arXiv preprint arXiv:1910.07461* (2019).